Kidney International, Vol. 64 (2003), pp. 923–932

Classification and rescue of ROMK mutations underlying hyperprostaglandin E syndrome/antenatal Bartter syndrome

Melanie Peters, Saskia Ermert, Nikola Jeck, Christian Derst, Ulla Pechmann, Stefanie Weber, Karl P. Schlingmann, Hannsjoerg W. Seyberth, Siegfried Waldegger, and Martin Konrad

Department of Pediatrics, Philipps University Marburg, Marburg, Germany; and Department of Physiology, Philipps University Marburg, Marburg, Germany

Classification and rescue of ROMK mutations underlying hyperprostaglandin E syndrome/antenatal Bartter syndrome.

Background. Mutations in the renal K^+ channel ROMK (Kir 1.1) cause hyperprostaglandin E syndrome/antenatal Bartter syndrome (HPS/aBS), a severe tubular disorder leading to renal salt and water wasting. Several studies confirmed the predominance of alterations of current properties in ROMK mutants. However, in most of these studies, analysis was restricted to nonmammalian cells and electrophysiologic methods. Therefore, for the majority of ROMK mutations, disturbances in protein trafficking remained unclear. The aim of the present study was the evaluation of different pathogenic mechanisms of 20 naturally occurring ROMK mutations with consecutive classification into mutational classes and identification of distinct rescue mechanisms according to the underlying defect.

Methods. Mutated ROMK potassium channels were expressed in *Xenopus* oocytes and a human kidney cell line and analyzed by two electrode voltage clamp analysis, immunofluorescence, and Western blot analysis.

Results. We identified 14 out of 20 ROMK mutations that did not reach the cell surface, indicating defective membrane trafficking. High expression levels rescued six out of 14 ROMK mutants, leading to significant K^+ currents. In addition, two early inframe stop mutations could be rescued by aminoglycosides, resulting in full-length ROMK and correct trafficking to the plasma membrane in a subset of transfected cells.

Conclusion. In contrast to previous reports, most of the investigated ROMK mutations displayed a trafficking defect that might be rescued by pharmacologic agents acting as molecular chaperones. The evaluation of different disease-causing mechanisms will be essential for establishing new and more specific therapeutic strategies for HPS/aBS patients.

Key words: ROMK, hyperprostaglandin E syndrome, antenatal Bartter syndrome, trafficking defect, mutational classification, aminoglycoside.

Received for publication May 16, 2002
and in revised form December 16, 2002
Accepted for publication April 17, 2003

The inwardly rectifying renal outer medullary K^+ channel ROMK (Kir 1.1) plays a critical role in renal salt reabsorption in the thick ascending limb of Henle's loop (TAL) [1, 2]. In the TAL, sodium chloride is reabsorbed in symport with K^+ via the bumetanide-sensitive Na^+-K^+-$2Cl^-$ cotransporter NKCC2. As the luminal K^+ concentration is low, a permanent K^+ recycling via ROMK is essential for proper function of NKCC2 [3, 4]. Consequently, mutations in both, *SLC12A1*, encoding NKCC2, and in *KCNJ1*, encoding ROMK, lead to hyperprostaglandin E syndrome/antenatal Bartter syndrome (HPS/aBS), a severe salt-losing tubular disorder with antenatal onset [5–7]. The clinical presentation of HPS/aBS patients is characterized by polyhydramnios leading to premature delivery, severe salt and water losses postnatally, hypokalemic alkalosis, hyperprostaglandinuria, and hypercalciuria associated with medullary nephrocalcinosis [8, 9].

Numerous mutations distributed all over the protein have been identified in patients with HPS/aBS, including nonconservative amino acid exchanges, premature stop mutations, and large deletions [5, 7, 10–14]. Until now, most of the missense mutations have been clustered in two regions (Fig. 1): (*1*) the channel core region (amino acids 84 to 180) and (*2*) the pH sensor, which depends on the cytosolic arginine/lysine/arginine (Arg/Lys/Arg) triad assembled by amino acid residues at positions 41, 80, and 311.

Mutations in the channel core region are thought to lead to defective K^+ conductance due to conformational changes [15], whereas mutations affecting the Arg/Lys/Arg triad cause a shift of the pH gating off the neutral range to more alkaline pH values [11]. However, many ROMK mutations do not affect these two regions; therefore, alternative pathogenic mechanisms have to be considered.

As shown for mutations in the cystic fibrosis transmembrane regulator (CFTR), five basic pathogenic mechanisms can be differentiated leading to a classification into five

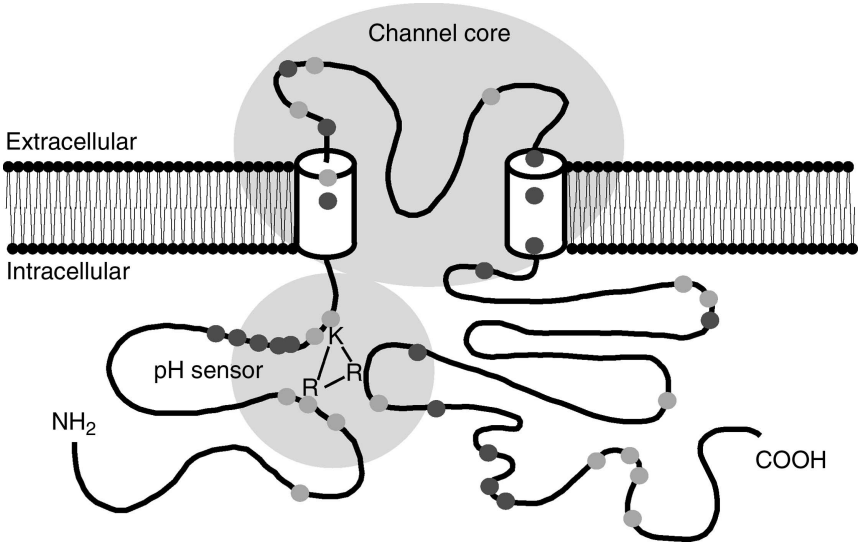

Fig. 1. Distribution of hyperprostaglandin E syndrome/antenatal Bartter syndrome (HPS/aBS) missense mutations in ROMK1. Mutations investigated in this study are indicated by dark gray circles. Most mutations cluster in the channel core region or in vicinity of the pH sensor domain.

mutational classes [16]: (*1*) class I mutations encompass premature stop-codons leading to a truncated mRNA transcript, (*2*) class II mutations lead to defective processing/trafficking, (*3*) class III mutations are characterized by disturbed regulation, (*4*) class IV encompasses mutations with decreased Cl^- currents (e.g., due to conformational changes), and (*5*) class V mutations lead to only small amounts of intact RNA due to splicing defects or due to mutations affecting the promotor. The identification and differentiation of these mechanisms is of special interest in view of pharmacologic attempts to restore protein function. Beside pharmacologic agents that act as molecular chaperones such as butyrates or glycerol for class II mutations [16, 17], aminoglycoside antibiotics have been shown to be effective in treating premature stop mutations (class I) in various genes, such as CFTR or dystrophin [18, 19]. Aminoglycosides cause extensive misreading of the RNA code by binding a specific site in ribosomal RNA and disturbing codon-anticodon recognition at the aminoacyl-tRNA acceptor site [20, 21]. Depending on the aminoglycoside, the surrounding context, and the stop mutation (UGA, UAA, or UAG), the synthesis of the full-length protein reached up to 25% of normal levels [18, 22]. A pilot study in cystic fibrosis patients carrying a premature stop mutation lead to significant repolarization of the nasal epithelium indicating chloride transport after topical application of gentamicin [23].

The aim of this study was the evaluation of different pathogenic mechanisms of 20 naturally occurring ROMK mutations in heterologous expression systems with consecutive classification into five mutational classes as prerequisites for new therapeutic approaches that are aimed at the restoration of protein function. The distribution of the investigated mutations is shown in Figure 1.

Following site-directed mutagenesis, ROMK1 constructs were analyzed in *Xenopus* oocytes by electrophysiologic methods and immunofluorescence. The results were subsequently confirmed in HEK293 cells. According to the underlying defects, we assigned the mutations investigated in our study and those ROMK mutations that had already been functionally analyzed before into five mutational classes and applied different techniques for restoration of protein function.

METHODS

Mutational analysis

Mutational analysis was performed in patients diagnosed as HPS/aBS who presented with the characteristic clinical triad of polyhydramnios, hyposthenuria/isosthenuria, and nephrocalcinosis. Genomic DNA was extracted from whole blood using standard methods and subsequently screened for mobility shifts by single-strand conformation polymorphism analysis (SSCA) [13]. Amplified DNA fragments that yielded aberrant band patterns were subsequently subjected to direct sequencing using the ALF express (Pharmacia Biotech, Freiburg, Germany). Mutations were confirmed by sequencing both strands from patient and parents.

Synthesis of ROMK1 constructs

For expression in *Xenopus* oocytes, rat ROMK1 (rROMK1) cDNA cloned into the polyadenylated pBF expression vector with a C-terminal flag epitope (a gift of B. Fakler, University of Freiburg, Germany) was used. Site-directed mutagenesis was performed using 23 to 25 oligomer nucleotide primers with the engineered nucleotide exchange in the center of the primer pairs (Quik Change™; Stratagene, La Jolla, CA, USA). The entire rROMK1 coding region was sequenced (ABI prism, Foster City, CA, USA).

Complementary RNA was transcribed in vitro in the presence of capping analog G (5′) ppp (5′) G using *Mlu*I linearized cDNA templates (SP6 mMessage Machine Kit; Ambion, Austin, TX, USA). After 15 minutes of DNase I treatment, cRNA was precipitated and purified by lithium chloride precipitation, as described by the manufacturer. Yield and concentration were measured spectrophotometrically (RNA/DNA calculator, GeneQuantII; Pharmacia Biotech, Freiburg, Germany) and by agarose gel electrophoresis.

For expression in HEK293 cells, human ROMK1 (hROMK1) tagged with an N-terminal HA-epitope was cloned in a pEGFP-C1 vector (Clontech, Palo Alto, CA, USA) and site-directed mutagenesis was performed, as described above. Again, mutants were verified by sequencing of the entire hROMK1 coding region.

Oocyte isolation and injection

Oocytes were obtained from female *Xenopus laevis* and defolliculated by incubation for 1 hour in modified ORII solution [82.5 mmol/L NaCl, 2 mmol/L KCl, 1 mmol/L $MgCl_2$ 1, 5 mmol/L N-2-hydroxyethylpiperazine-N′-2-ethanesulfonic acid (HEPES), pH 7.5] containing 2 mg/mL collagenase A (Roche Molecular Biochemicals, Mannheim, Germany). Stages V and VI oocytes were selected and stored at 16°C in ND96 solution (96 mmol/L NaCl 96, 2 mmol/L KCl, 1.8 mmol/L $CaCl_2$, 1 mmol/L $MgCl_2$, 5 mmol/L HEPES, pH 7.5) supplemented with 20 μg/mL gentamicin, 0.5 mmol/L theophylline, and 2.5 mmol/L sodium pyruvate. Defolliculated oocytes were injected with 50 nL water containing 0.1 ng and 1 ng cRNA and incubated 2 to 3 days at 16°C.

Immunostaining of mutant ROMK in *Xenopus* oocytes

After removal of the vitellin membranes, oocytes were fixed in Dent's fixative [20% methanol in dimethyl sulfoxide (DMSO)] at −20°C overnight. Oocytes were then incubated for 3 hours at room temperature or at 4°C overnight with the M2 anti-Flag antibody (Sigma Chemical Co., St. Louis, MO, USA) and washed with phosphate-buffered saline (PBS) for 2 to 3 hours. Subsequently, all oocytes were incubated with a Cy3-conjugated secondary antibody (Dianova, Hamburg, Germany). Stained oocytes were fixed with 3.7% paraformaldehyde, embedded with Technovit 7100 (Heraeus Kulzer, Wehrheim, Germany) and cut to 4 μm sections. Analysis was performed with a fluorescence microscope (Leica DMRB, Wetzlar, Germany) and with the Leica QWin software.

Electrophysiology

Two to three days after injection, two-electrode voltage clamp measurements were performed at room temperature with a GeneClamp 500 amplifier (Axon Instruments, Union City, CA, USA). Currents were recorded in KD96 solution (89 mmol/L KCl, 1.8 mmol/L $CaCl_2$, 1 mmol/L $MgCl_2$, 5 mmol/L HEPES, pH 7.4) during voltage ramps from –20 mV to +20 mV (holding potential at 0 mV). Data from at least two different batches of oocytes are shown. Statistical analysis was performed on seven or more oocytes derived from one preparation. The error bars in the diagram were calculated from the standard error of mean (SEM).

Immunostaining of mutant ROMK in HEK293 cells

HEK293 cells were grown in Earle's minimal essential medium (MEM) supplemented with 10% fetal calf serum, penicillin/streptomycin, L-glutamine, and nonessential amino acids on 8-well LabTeks for immunocytochemistry (Nalge Nunc International, Rochester, MN, USA). Subsequently, cells were transfected with 0.5 to 0.8 μg of mutant and wild-type hROMK cDNA as described by the manufacturer (TransFast; Promega, Madison, WI, USA).

Chemical treatment

Cells for aminoglycoside treatment were grown as described above. After transfection, G-418 (PAA Laboratories, Germany) or gentamicin (Gibco, Invitrogen Diagnostics, Karlsruhe, Germany) was added to the growth medium at the indicated concentrations. After 18 to 22 hours' incubation time, HEK293 cells were analyzed by confocal microscopy and Western blot.

Confocal microscopy

Laser-scanning confocal microscopy was used to determine the cellular localization of pEGFP-ROMK wild-type and mutants in HEK293 cells. The localization was visualized with the Olympus Fluoview confocal laser-scanning microscope (Olympus Optical BX50WI, Hamburg, Germany) and analyzed by cutting 7 to 11 sections at a distance of 0.5 to 1 μm using FluoView 2.1 software.

Western blot analysis

For Western blot analysis, HEK 293 cells were lysed in Laemmli sample buffer and heated at 95°C for 5 minutes. Subsequently, proteins were separated by 12% sodium dodecyl sulfate (SDS) gel electrophoresis and transferred to a nitrocellulose membrane (Hybond-C Extra, Amersham Life Science, Freiburg, Germany). After blocking in 5% milk overnight, the blot was incubated with anti-HA 1:800 (Roche Diagnostics, Mannheim, Germany) and a horseradish peroxidase-conjugated secondary antibody 1:2000 (Amersham Bioscience, UK). Detection was carried out using a chemiluminescence kit (ECL+; Amersham Biosciences, Buckinghamshire, UK) according to the manufacturer's instructions.

RESULTS

Mutational analysis

In addition to 13 ROMK mutations that had been published previously [7, 11, 13], six new mutations, T71M,

Table 1. Characterization of the new ROMK mutations

Patient	Mutation	Nucleotide exchange	Homozygous/ heterozygous
1	T71M[a]	ACG>ATG	Homozygous
2	Y79H[a]	TAC>CAC	Heterozygous
	insCpos353>362X		Heterozygous
3	F95S[a]	TTT>TCT	Heterozygous
	delAAAGpos332>368X		Heterozygous
4	A177T[a]	GCC>ACC	Homozygous
5	A306T[a]	GCT>ACT	Heterozygous
6	Y314C[a]	TAT>TGT	Heterozygous
	R311W	CGG>TGG	Heterozygous

[a] Indicates new ROMK mutations which are investigated in this study; nucleotides are numbered according to their position in hROMK1

Y79H, F95S, A177T, A306T, and Y314C (for detailed information, see Table 1) were identified in patients who exhibited the typical clinical features of HPS/aBS. Except for A177T, all point mutations affect amino acid positions that are highly conserved among the inwardly rectifying K^+ channels family.

Mutations were discerned from polymorphisms by demonstration of their absence in 100 control chromosomes and by cosegregation with the disease phenotype within the families.

ROMK distribution in *Xenopus* oocytes

To study the subcellular localization of wild-type and mutant ROMK protein, immunostaining of oocytes was performed. Positive membrane staining was shown in oocytes expressing ROMK wild-type (Fig. 2A), whereas no membrane staining was observed in water-injected oocytes (Fig. 2B).

Membrane staining was also observed for F95S, A156V, A177T, and R311W after injection of 0.1 ng cRNA (Fig. 2C).

In contrast, no membrane localization after injection of 0.1 ng cRNA was detected for T71M, V72E, D74Y, W77X, Y79X, Y79H, D108H, V122E, G167E, A198T, L220F, A306T, Y314C, L320P, R324L, and F325C, which were retained exclusively in the cytosolic compartment (Fig. 2D).

Electrophysiology

The electrophysiologic properties of the ROMK mutations were analyzed by heterologous expression in *Xenopus* oocytes and two-electrode voltage clamp analysis. As reported previously, expression of 0.1 ng wild-type ROMK cRNA in *Xenopus* oocytes gave rise to weakly inwardly rectifying potassium currents [11]. Strongly reduced current amplitudes were observed for all mutations tested in this study after expression of 0.1 ng cRNA (Fig. 3).

Immunostaining of ROMK mutations in HEK293 cells

To study the subcellular localization of the ROMK mutants in a mammalian kidney cell line, transfection of

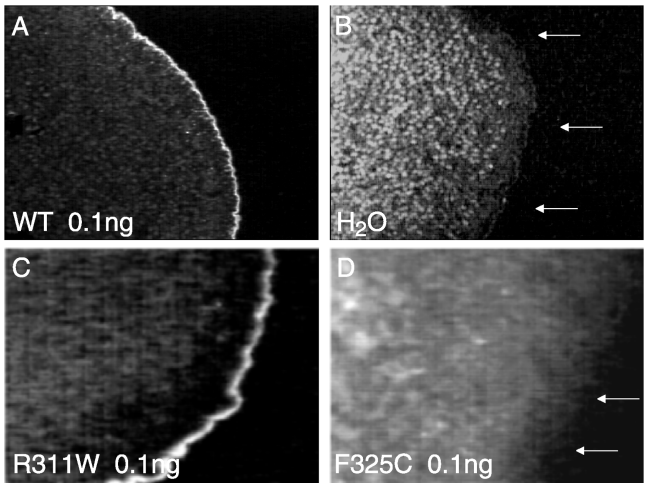

Fig. 2. Examples of oocytes injected with 0.1 ng cRNA. Correct insertion in the oocyte membrane is shown in wild-type (WT)-ROMK expressing oocytes (*A*) and the R311W mutant *(C)*. In contrast, negative staining is demonstrated in water (H_2O)-injected oocytes (*B*) and F325C *(D)*, indicating intracellular retention of this mutant. Arrows indicate the plasma membrane.

mutations in HEK293 cells was performed. As expected, membrane staining was observed for the ROMK wild-type (Fig. 4A), whereas for the early inframe stop mutation W77X only intracellular staining was detected (Fig. 4B).

Analogously to the expression in *Xenopus* oocytes, membrane staining was shown for the F95S, A156V, A177T, and R311W (Fig. 4C).

In contrast, no membrane staining was observed for the following mutations: T71M, V72E, D74Y, Y79H, D108H, V122E, G167E, A198T, A306T, L320P, R324L, and F325C, confirming the results obtained in oocytes (Fig. 4D).

The results of the functional analysis and immunofluorescence in *Xenopus* oocytes and immunofluorescence in HEK293 cells are summarized in Table 2.

Rescue of trafficking mutations (class II) by overexpression

As mentioned before, the ROMK mutations T71M, Y79H, A198T, L220F, A306T, and R324L were not visible in the plasma membrane after injection of 0.1 ng cDNA. Increasing expression levels of the mutated ROMK proteins, however, induced a partial restoration of membrane trafficking. After injection of the tenfold excess of cRNA (1 ng), positive membrane staining was detected indicating forced routing to the membrane (Fig. 5). In contrast, overexpression of the remaining mutants did not result in correct membrane insertion.

After injection of 0.1 ng cRNA, the ROMK mutations T71M, Y79H, A198T, L220F, A306T, and R324L showed no or only low potassium currents. In parallel to increased membrane localization after injection of 1 ng cRNA, we

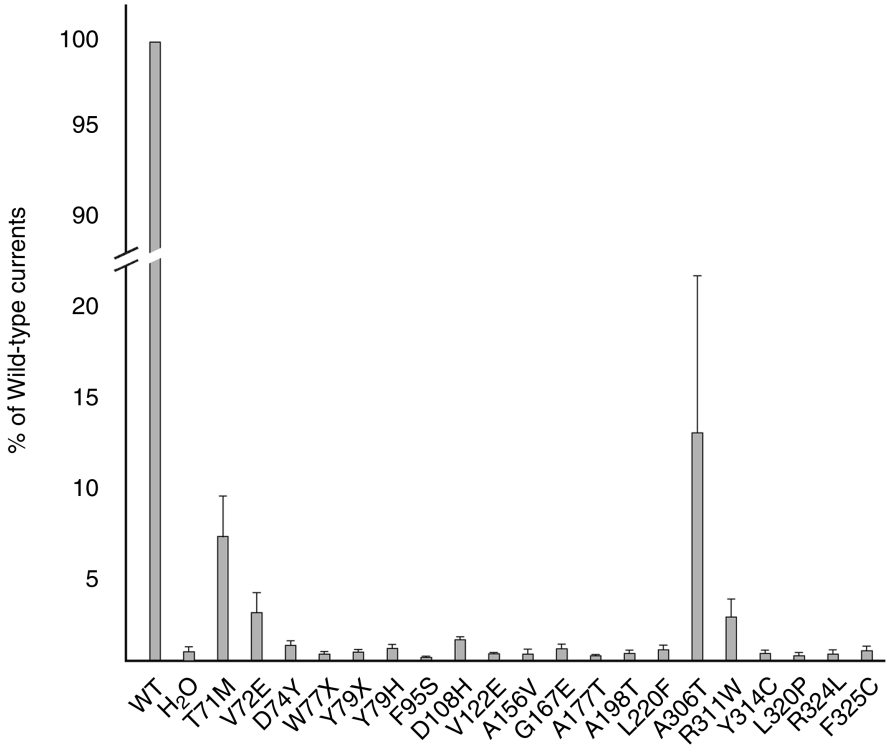

Fig. 3. Functional analysis of 20 ROMK mutations after expression of 0.1 ng cRNA. Current amplitudes were measured at a voltage step of –10 mV at an ambient K^+ concentration of 98 mmol/L, pH 7.4. Data are given as mean ± SEM.

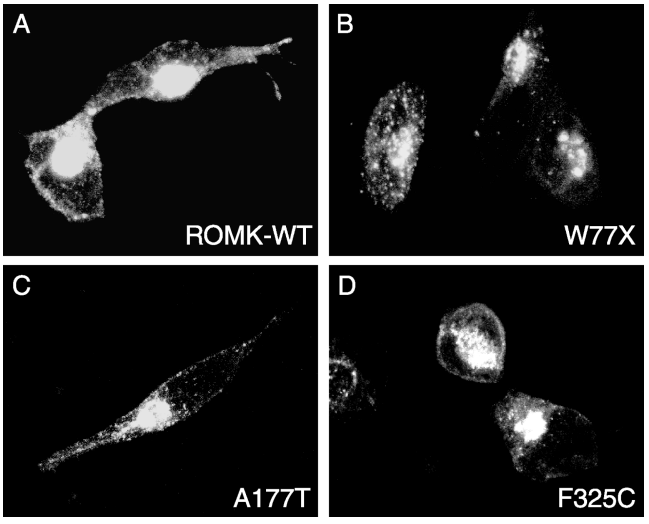

Fig. 4. Examples of ROMK expression of each group in HEK293 cells. A membrane negative staining pattern is demonstrated for an early stop mutation W77X (*B*), and F325C *(D)*, whereas staining in the plasma membrane is shown in ROMK-wild-type (WT) expressing HEK293 cells (*A*) and A177T *(C)*. Confocal images obtained from 5 to 11 optic sections are shown.

observed a significant increase ($P < 0.05$) in functional expression: 86% ± 9% for T71M, 20% ± 4.5% for Y79H, 14% ± 3.5% for A198T, 29% ± 3% for L220F, 71% ± 4.5% for A306T, and 26% ± 4.5% for R324L of wild-type currents ($N > 7$) (Fig. 6).

Overexpression of wild-type ROMK cRNA rapidly killed oocytes within the first 24 hours; therefore, all results obtained were referred to the wild-type currents obtained after injection of 0.1 ng cRNA.

Rescue of preterm stop mutations (class I) after application of aminoglycosides

To determine whether aminoglycosides could lead to a suppression of spurious preterm stop-codons in ROMK, HEK293 cells transfected with W77X and Y79X cDNA were grown in the presence of gentamicin and G-418 at the indicated concentrations. As expected, no full-length protein could be detected in protein preparations from control cells. However, a 73 kD band corresponding to the full-length protein (+GFP) appeared after incubation of 0.1 to 0.2 μg/mL gentamicin and 0.05 to 0.15 μg/mL G-418 (Fig. 7).

Immunofluorescence analysis of aminoglycoside-treated cell cultures revealed a positive membrane staining in a subset of transfected HEK293 cells. Depending on the stop-mutation and the aminoglycoside concentration, about 5% to 10% of transfected cells showed a positive membrane staining with a slightly higher rate for W77X than for Y79X as estimated by confocal microscopy. In addition, aminoglycoside treatment significantly changed the immunofluorescence pattern. The truncated proteins in absence of aminoglycosides were solely restricted to a small area around the nuclei probably reflecting the endoplasmic reticulum, whereas a more diffuse distribution within the

Table 2. Summary of the electrophysiologic and immunofluorescent results with subsequent classification into mutational classes (adopted from [16])

	Membrane staining 0.1 ng (oocyte)	Membrane staining 1 ng (oocyte)	Currents 0.1 ng (oocyte)	Currents 1 ng (oocyte)	Membrane staining (HEK293)	Mutational class
WT	+	+	+	+	+	
W77X	−	−	−	−	−	I
Y79X	−	−	−	−	−	I
V72E	−	−	−	−	−	II
D74Y	−	−	−	−	−	II
D108H	−	−	−	−	−	II
V122E	−	−	−	−	−	II
G167E	−	−	−	−	−	II
Y314C	−	−	−	−	−	II
L320P	−	−	−	−	−	II
F325C	−	−	−	−	−	II
T71M	−	+	(+)	+	−	II+ rescue
Y79H	−	+	−	+	−	II+ rescue
A198T	−	+	−	+	−	II+ rescue
L220F	−	+	−	+	−	II+ rescue
A306T	−	+	−	+	−	II+ rescue
R324L	−	+	−	+	−	II+ rescue
F95S	±	±	−	−	±	III/IV
A156V	±	±	−	−	±	III/IV
A177T	±	±	−	−	±	III/IV
R311W	±	±	−	−	±	III

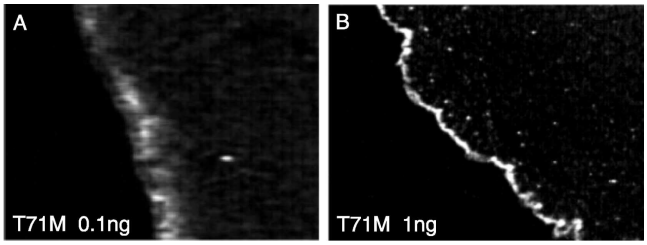

Fig. 5. Oocytes injected with 0.1 ng (*A*) and 1 ng cRNA (*B*) are shown with negative membrane staining after expression of 0.1 ng cRNA and positive membrane-staining after injection of the tenfold excess of cRNA.

cell was observed after application of aminoglycosides, possibly reflecting escape from the endoplasmic reticulum and further transport to the Golgi (Fig. 8).

DISCUSSION

This study examined six new ROMK mutations and 13 of 37 ROMK mutations that have been described before [5, 7, 10–14]. The distribution of these mutations within the N-terminus, the channel core region, and the C-terminus of ROMK implies different pathogenic mechanisms, including (*1*) a fundamental disturbance of the pore forming components with impaired K^+ conductance, (*2*) defective regulation of ROMK, and/or (*3*) a disturbed processing or trafficking to the cell surface. In addition, also inframe stop mutations resulting in truncated proteins and mutations disturbing the promoter region have been described [5, 7, 10, 24].

Considering the electrophysiologic and immunofluorescent results of expression in *Xenopus* oocytes and HEK293 cells, four different groups of ROMK mutations were distinguished.

The first group consisted of F95S, A156V, A177T, and R311W that reached the plasma membrane both in *Xenopus* oocytes and HEK293 cells, but showed no functional expression under physiologic conditions. Analogous to the CFTR-classification mentioned before, these mutations can be assigned to class III/IV, two classes which have been shown to be difficult to repair (class III) or only by combining different pharmacologic agents (class IV) [16].

The pathogenic mechanism of R311W was described previously and was shown to be associated with disturbances in the pH-dependent gating of ROMK [11]. Since mutations at amino acid position 95, 156, and 177 are located within the two transmembrane domains, a disturbance of the pH gating seems unlikely. The decreased K^+ conductance of these mutants might either result from conformational changes of the pore forming domains or a disturbed assembly, which has been shown to require multiple interaction sites in the core region and cytoplasmic termini of ROMK [25].

The second group consisted of V72E, D74Y, D108H, V122E, G167E, Y314C, L320P, and F325C. Mutations of this group showed a disturbed trafficking to the plasma membrane and no functional expression in electrophysiologic recordings. Mutations of this group could not be rescued by overexpression of the protein.

Concerning the expression of the V72E and V122E mutants, differing results in the electrophysiologic recordings and immunofluorescence in *Xenopus* oocytes have been shown by Starremans et al [14]. Differences in the immunofluorescence might either arise from dif-

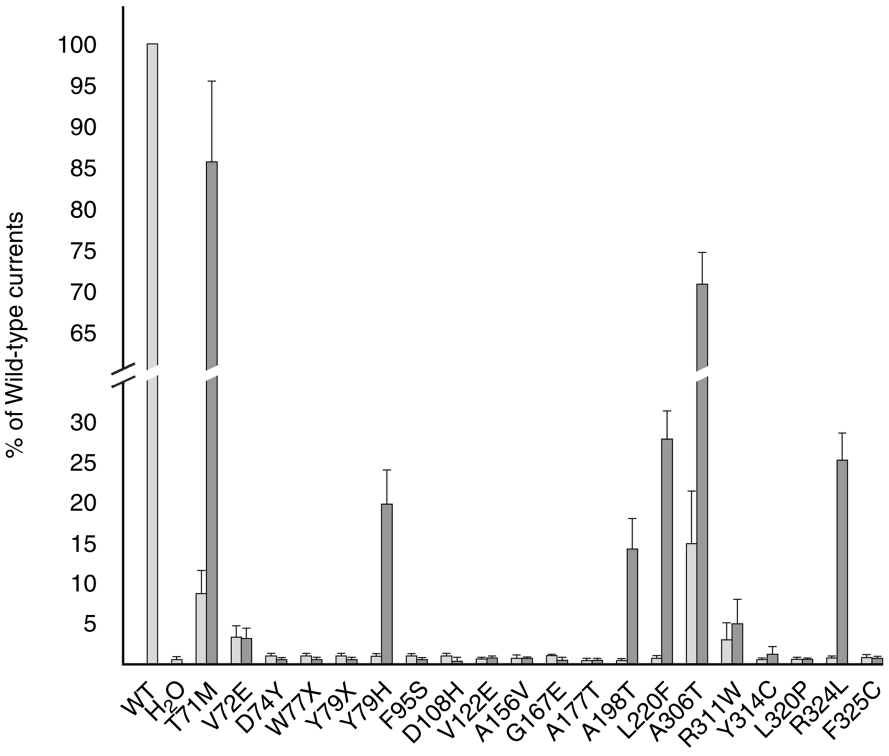

Fig. 6. Functional analysis of 20 ROMK mutations after expression of 0.1 ng (□) and 1 ng (■) cRNA. Current amplitudes were measured at a voltage step of –10 mV at an ambient K^+ concentration of 98 mmol/L, pH 7.4. Data are given as mean ± SEM.

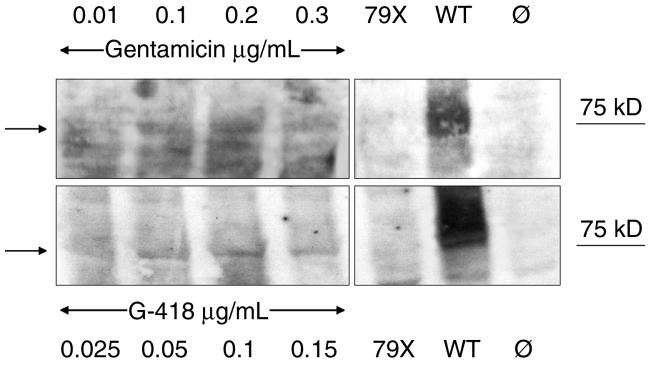

Fig. 7. Western blot analysis of ROMK Y79X after treatment with gentamicin and G-418 after 22 hours incubation time. Ø indicates untransfected HEK cells.

ferent sections selected from opposite hemispheres of the oocytes or from the use of different splice forms of the ROMK protein that might also explain the differing electrophysiologic results. We used ROMK1 in our study, whereas the ROMK2 splice form, which lacks the first 19 residues compared to ROMK1, was used in the study from Starremans et al [14]. Therefore, an additional influence of the first residues on trafficking and functional expression of ROMK in *Xenopus* oocytes cannot be ruled out. However, as already shown by Derst et al [15], mutations that are located near the transmembrane domains or the core region (amino acids 84 to 180) completely abolish functional expression, whereas mutations in the N- and C-termini only partially reduce current amplitudes, which is also confirmed by our results. None of our ROMK mutations, which are located around the core region, exhibited any functional expression, neither after expression of 0.1 ng or 1 ng cRNA as demonstrated in Figure 6.

In this group, an impaired trafficking to the cell surface was shown, which might result from either defective protein folding leading to prolonged endoplasmic reticulum–chaperone binding and degradation or disturbed endoplasmic reticulum retentions signals. Endoplasmic reticulums export signals have recently been described in the C-terminal domain of Kir2 and Kir3 channels [26–28]. C-terminal truncation or substitution with homologous regions from Kir channels containing no export signal strongly reduced or completely abolished surface expression of these Kir subunits. Therefore, it is not surprising that several C-terminal ROMK mutations also show trafficking defects. Interestingly, transferring the ROMK C-terminal domain (but not the C-terminus of Kir3.1, Kir3.4, Kir6.1, and Kir6.2) to Kir2.1 channels was still capable with plasma membrane expression, indicating that the ROMK C-terminus may harbor endoplasmic reticulum export signals [26].

The third group comprises T71M, Y79H, A198T, L220F, A306T, and R324L that could be successfully rescued by overexpression and overwhelming the cellular quality control machinery of oocytes by a tenfold excess of cRNA. This group showed no functional ex-

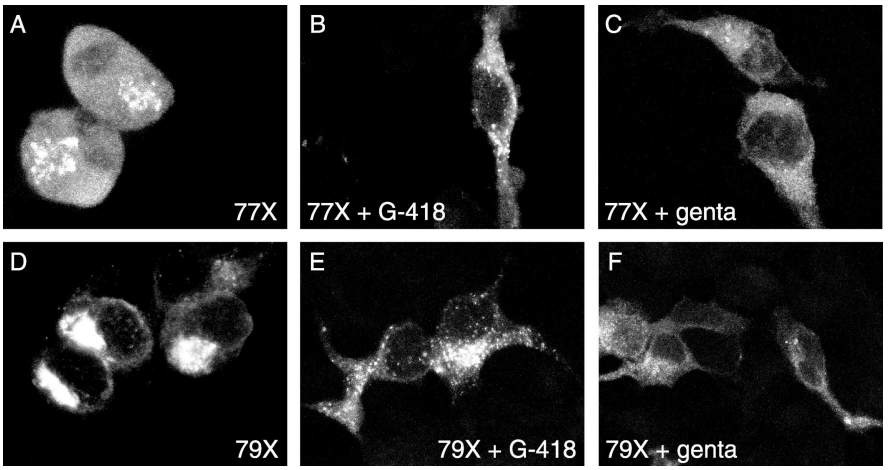

Fig. 8. Expression of ROMK W77X (*A* to *C*) and Y79X (*D* to *F*) in HEK293 cells before and after treatment with gentamicin (genta) and G-418 after 18 to 22 hours incubation time.

pression after expression of 0.1 ng cRNA but a restoration of K^+ currents to 14% to 86% of wild-type currents after expression of 1 ng cRNA.

Forced routing to the plasma membrane by overexpression has already been shown before for three ROMK mutations and mutant aquaporin-2 water channels involved in nephrogenic diabetes insipidus, indicating intracellular retention mechanisms [14, 29]. It appears that these point mutations can alter protein conformation in a way that affects solely the trafficking but not the protein function, as no fundamental disturbance of the K^+ conductance characteristics occurred. This finding could have important implications in terms of strategies to correct some of the ROMK mutations in HPS/aBS patients. Pharmacologic rescue that permits plasma membrane localization might be sufficient to correct proper ion channel function, even if the perfect native conformation is not achieved.

Concerning A198T, differering results were observed compared to the study of Starremans et al [14] who found approximately 85% of wild-type currents after expression of 25 pg of A198T cRNA (which corresponds to A179T in hROMK2) with positive membrane staining in *Xenopus* oocytes. However, we did not detect membrane staining or functional expression at low expression levels. This result is in accordance with observations of Derst et al [15], and Schulte and Fakler [30] who showed very low or absent functional expression of A198T.

Interestingly, for ROMK-L220F, a pH-dependent gating was shown from Schulte et al [11]. This result might combine the effects of impaired processing at low expression levels, on one hand, and a regulation defect after overexpression, on the other hand, leading to only partial K^+ currents under physiologic pH conditions as observed in our study. Similarly, combined mechanisms must be postulated for the T71M, Y79H, A198T, A306T, and R324L mutants that also show only partial K^+ currents compared to the wild-type after overexpression in oocytes. Beside pH shifting effects, as already discussed for the L220F, additional regulatory mechanisms might be disturbed in the remaining mutations of this group such as adenosine triphosphate (ATP)-binding or phosphorylation.

The structural integrity of N- and C-terminal domains has been shown for ROMK [11] as well as for other Kir subunits [31, 32]. Mutations in either part may have profound structural effect on the entire cytosolic domain of Kir channels. In addition, due to the three-dimensional structure, functional important domains are often distributed over the entire cytosolic domain (e.g., multiple N- and C-terminal endoplasmic reticulum export motifs, pH sensor, or multiple interaction sites for assembly) [11, 25, 27]. Therefore, multiple pathophysiologic mechanisms resulting from a single mutation, like reduced membrane expression and disturbed pH gating of ROMK, might be explained by a severe structural disturbance in the cytosolic domains.

The fourth group encompasses two preterm stop mutations W77X and Y79X that are susceptible to suppression by aminoglycosides. As shown before, aminoglycoside binding is thought to induce a conformational change at the decoding site that leads to a reduction in proofreading with an increase of misincorporation of near-cognate aminoacyl-tRNAs [33]. The substitution is not fully effective leading to restoration of only a small fraction of normal levels of wild-type transcripts [34]. In former studies, it has been shown that, depending on the aminoglycoside, the identity of the stop-codon and its sequence context, about 20% to 25% of wild-type-levels are achievable [18, 35, 36]. In our study, we found about 5% to 10% of wild-type-levels in Y79X, and about 10% to 20% in W77X, as estimated by the confocal microscopy/immunofluorescence. These results are comparable to the study of Keeling and Bedwell [22], showing

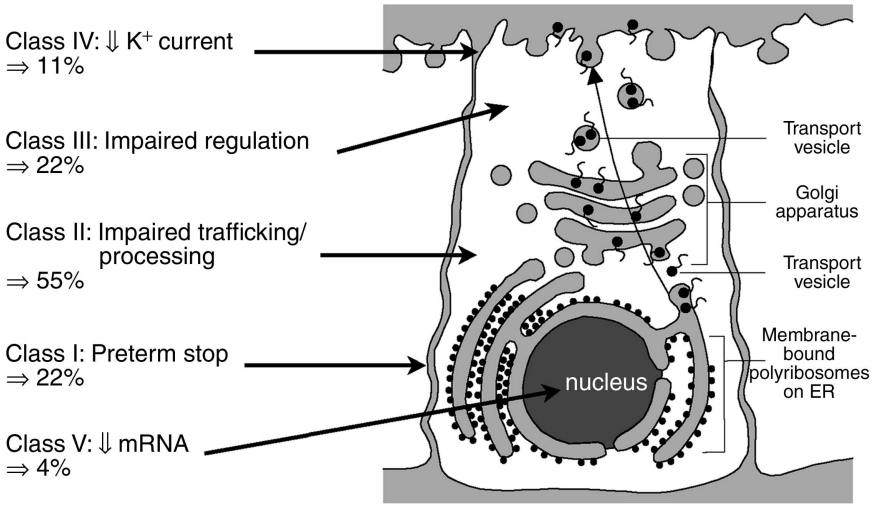

Fig. 9. Classification into five mutational classes (adopted from [16]), according to the underlying defect and assignment of the ROMK mutations investigated in our study together with ROMK mutations that had been clarified before [10, 11, 24] into these classes.

that the tetranucleotide UGA/C (W77X) is more readily suppressed than UAG/A (Y79X) by gentamicin in a mammalian translation system. However, only a small fraction of suppressed ROMK preterm stop mutations displayed a positive membrane staining in our study (see Fig. 8), which has also been shown before by others [37]. In their study, Bedwell et al [37] found that, after incubation of CFTR-W1282X with G-418, full-length CFTR was expressed. However, they were unable to detect the repaired protein at the apical membrane without further cyclic adenosine monophosphate (cAMP) stimulation indicating that G-418 restored first the expression of full-length CFTR and that the resulting functional protein was trafficked to the apical membrane after cAMP stimulation in a second step. As the ribosome is introducing not only the original tRNA but also missense mutations, an impaired trafficking to the cell membrane in a subset of suppressed proteins is presumable. However, even partial restoration of ROMK function might be sufficient to effectively alleviate the disease phenotype.

In contrast to premature translation termination codons introduced by mutations, naturally occurring termination codons are thought to lie within a context that promotes efficient translation termination [23], as recognition of translation termination signals is not only limited to the trinucleotide codons UGA, UAG, UAA. It is, instead, recognized by an extended tetranucleotide termination signal composed of the stop-codon and the first nucleotide that follows (e.g., purine nucleotides following the stop promote translation termination more efficiently than stop-codons followed by pyrimidines) [22, 38]. Therefore, naturally occurring stop mutations might be protected more effectively by a special environment than stop-codons introduced by mutations. This is confirmed by former studies showing no significant side effects after treatment with G-418 in cell culture experiments [18] or gentamicin in a clinical study [23].

Analogous to the classification of CFTR mutations [16], we assigned the ROMK mutations investigated in our study into the five mutational classes (see also Table 2). Together with those ROMK mutations that have already been functionally analyzed before, more than 50% of the ROMK mutations show a trafficking defect (Fig. 9).

Thus, defective ROMK processing seems to be the predominant pathogenic mechanism leading to HPS/aBS, which is most favorable in terms of new pharmacologic approaches that aim at the rescue of the mistrafficked protein. Thus, in ROMK-mutations, butyrates or specific ROMK agonists/antagonists might also overcome the trafficking defects of class II mutations, whereas certain aminoglycosides might be useful for ROMK stop mutations of class I.

Loss-of-function mutations have also been described in other members of the Kir family, such as the Kir6.1 associated with familial persistent hyperinsulinemic hypoglycaemia of infancy [39] and the Kir2.1 leading to Andersen syndrome, which is characterized by periodic paralysis, cardiac arrhythmias, and dysmorphic features. Although no detailed functional characterization is available for the Kir2.1 mutations, it is tempting to speculate that several mutations in the N- and C-terminal region might also affect membrane trafficking. Therefore, identification of different pathophysiologic mechanisms in ROMK and pharmacologic restoration of trafficking mutations or inframe stop mutations might have significant implication for treatment of other defective members of the Kir family [40].

ACKNOWLEDGMENTS

We would like to thank the physicians who provided us with patients' DNA and clinical information. We also thank Uwe Schulte and Karen Wild, Eberhard-Karls-University of Tübingen for help with the immunohistochemistry, Michael Bette, Philipps-University Marburg for help with the confocal microscopy, and Petra Waldegger for excellent technical assistance. This study was supported by grants of the Deutsche Forschungsgemeinschaft (Ko1480/3-2, Wa1088/3-1), Kempkes Stiftung Marburg, and Aventis.

Reprint requests to Martin Konrad, M.D., Department of Pediatrics, Philipps-University Marburg, Deutschhausstrasse 12, D-35037 Marburg, Germany.
E-mail: konradm@mailer.uni-marburg.de

REFERENCES

1. Giebisch G, Wang W: Potassium transport: From clearance to channels and pumps. *Kidney Int* 49:1624–1631, 1996
2. Hebert SC, Wang WH: Structure and function of the low conductance KATP channel, ROMK. *Wien Klin Wochenschr* 109:471–476, 1997
3. Greger R: Ion transport mechanisms in thick ascending limb of Henle's loop of mammalian nephron. *Physiol Rev* 65:760–797, 1985
4. Boim MA, Ho K, Shuck ME, *et al*: ROMK inwardly rectifying ATP-sensitive K+ channel. II. Cloning and distribution of alternative forms. *Am J Physiol* 268(6 Pt 2): F1132–F1140, 1995
5. Simon DB, Karet FE, Rodriguez-Soriano J, *et al*: Genetic heterogeneity of Bartter's syndrome revealed by mutations in the K+ channel. ROMK. *Nat Genet* 14:152–156, 1996
6. Simon DB, Karet FE, Hamdan JM, *et al*: Bartter's syndrome, hypokalaemic alkalosis with hypercalciuria, is caused by mutations in the Na-K-2Cl cotransporter NKCC2. *Nat Genet* 13:183–188, 1996
7. The International Study Group for Bartter-like Syndromes: Mutations in the gene encoding the inwardly-rectifying renal potassium channel, ROMK, cause the antenatal variant of Bartter syndrome: evidence for genetic heterogeneity. *Hum Mol Genet* 6:17–26, 1997
8. Reinalter SC, Jeck N, Brochhausen C, *et al*: Role of cyclooxygenase-2 in hyperprostaglandin E syndrome/antenatal Bartter syndrome. *Kidney Int* 62:253–260, 2002
9. Peters M, Jeck N, Reinalter S, *et al*: Clinical presentation of genetically defined patients with hypokalemic salt-losing tubulopathies. *Am J Med* 112:183–190, 2002
10. Feldmann D, Alessandri JL, Deschenes G: Large deletion of the 5′ end of the ROMK1 gene causes antenatal Bartter syndrome. *J Am Soc Nephrol* 9:2357–2359, 1998
11. Schulte U, Hahn H, Konrad M, *et al*: pH gating of ROMK (K(ir)1.1) channels: Control by an Arg-Lys-Arg triad disrupted in antenatal Bartter syndrome. *Proc Natl Acad Sci USA* 96:15298–15303, 1999
12. Kunzelmann K, Hubner M, Vollmer M, *et al*: A Bartter's syndrome mutation of ROMK1 exerts dominant negative effects on K(+) conductance. *Cell Physiol Biochem* 10:117–124, 2000
13. Jeck N, Derst C, Wischmeyer E, *et al*: Functional heterogeneity of ROMK mutations linked to hyperprostaglandin E syndrome. *Kidney Int* 59:1803–1811, 2001
14. Starremans PF, van Der Kemp AM, Knoers NM, *et al*: Functional implications of mutations in the human renal outer medullary potassium channel (ROMK2) identified in Bartter syndrome. *Pflugers Arch* 443:466–472, 2002
15. Derst C, Konrad M, Köckerling A, *et al*: Mutations in the ROMK gene in antenatal Bartter syndrome are associated with impaired K+ channel function. *Biochem Biophys Res Commun* 230:641–645, 1997
16. Zeitlin PL: Novel pharmacologic therapies for cystic fibrosis. *J Clin Invest* 103:447–452, 1999
17. Sato S, Ward CL, Krouse ME, *et al*: Glycerol reverses the misfolding phenotype of the most common cystic fibrosis mutation. *J Biol Chem* 271:635–638, 1996
18. Howard M, Frizzell RA, Bedwell DM: Aminoglycoside antibiotics restore CFTR function by overcoming premature stop mutations. *Nat Med* 2:467–469, 1996
19. Barton-Davis ER, Cordier L, Shoturma DI, *et al*: Aminoglycoside antibiotics restore dystrophin function to skeletal muscles of mdx mice. *J Clin Invest* 104:375–381, 1999
20. Burke JF, Mogg AE: Suppression of a nonsense mutation in mammalian cells in vivo by the aminoglycoside antibiotics G-418 and paromomycin. *Nucleic Acids Res* 13:6265–6272, 1985
21. Kaufman RJ: Correction of genetic disease by making sense from nonsense. *J Clin Invest* 104:367–368, 1999
22. Keeling KM, Bedwell DM: Clinically relevant aminoglycosides can suppress disease-associated premature stop mutations in the IDUA and P53 cDNAs in a mammalian translation system. *J Mol Med* 80:367–376, 2002
23. Wilschanski M, Famini C, Blau H, *et al*: A pilot study of the effect of gentamicin on nasal potential difference measurements in cystic fibrosis patients carrying stop mutations. *Am J Respir Crit Care Med* 161:860–865, 2000
24. Flagg TP, Tate M, Merot J, Welling PA: A mutation linked with Bartter's syndrome locks Kir 1.1a (ROMK1) channels in a closed state. *J Gen Physiol* 114:685–700, 1999
25. Koster JC, Bentle KA, Nichols CG, Ho K: Assembly of ROMK1 (Kir 1.1a) inward rectifier K+ channel subunits involves multiple interaction sites. *Biophys J* 74:1821–1829, 1998
26. Ma D, Zerangue N, Lin YF, *et al*: Role of ER export signals in controlling surface potassium channel numbers. *Science* 291:316–319, 2000
27. Ma D, Zerangue N, Raab-Graham K, *et al*: Diverse trafficking patterns due to multiple traffic motifs in G protein-activated inwardly rectifying potassium channels from brain and heart. *Neuron* 33:715–729, 2002
28. Stockklausner C, Ludwig J, Ruppersberg JP, Klocker N: A sequence motif responsible for ER export and surface expression of Kir2.0 inward rectifier K(+) channels. *FEBS Lett* 493:129–133, 2001
29. Kamsteeg EJ, Deen PM, van Os CH: Defective processing and trafficking of water channels in nephrogenic diabetes insipidus. *Exp Nephrol* 8:326–331, 2000
30. Schulte U, Fakler B: Gating of inward-rectifier K+ channels by intracellular pH. *Eur J Biochem* 267:5837–5841, 2000
31. Tucker SJ, Ashcroft FM: Mapping of the physical interaction between the intracellular domains of an inwardly rectifying potassium channel, Kir6.2. *J Biol Chem* 274:33393–33397, 1999
32. Jones PA, Tucker SJ, Ashcroft FM: Multiple sites of interaction between the intracellular domains of an inwardly rectifying potassium channel, Kir6.2. *FEBS Lett* 508:85–89, 2001
33. Pape T, Wintermeyer W, Rodnina M: Induced fit in initial selection and proofreading of aminoacyl-tRNA on the ribosome. *EMBO J* 18:3800–3807, 1999
34. Mankin AS, Liebman SW: Baby, don't stop! *Nat Genet* 23:8–10, 1999
35. Howard MT, Shirts BH, Petros LM, *et al*: Sequence specificity of aminoglycoside-induced stop condon readthrough: Potential implications for treatment of Duchenne muscular dystrophy. *Ann Neurol* 48:164–169, 2000
36. Du M, Jones JR, Lanier J, *et al*: Aminoglycoside suppression of a premature stop mutation in a Cftr−/− mouse carrying a human CFTR-G542X transgene. *J Mol Med* 80:595–604, 2002
37. Bedwell DM, Kaenjak A, Benos DJ, *et al*: Suppression of a CFTR premature stop mutation in a bronchial epithelial cell line. *Nat Med* 3:1280–1284, 1997
38. Manuvakhova M, Keeling K, Bedwell DM: Aminoglycoside antibiotics mediate context-dependent suppression of termination codons in a mammalian translation system. *RNA* 6:1044–1055, 2000
39. Thomas P, Ye Y, Lightner E: Mutation of the pancreatic islet inward rectifier Kir6.2 also leads to familial persistent hyperinsulinemic hypoglycemia of infancy. *Hum Mol Genet* 5:1809–1812, 1996
40. Plaster NM, Tawil R, Tristani-Firouzi M, *et al*: Mutations in Kir2.1 cause the developmental and episodic electrical phenotypes of Andersen's syndrome. *Cell* 105:511–519, 2001